Grounding Motivation in Energy Autonomy: A Study of Artificial Metabolism Constrained Robot Dynamics

Robert Lowe[1], Alberto Montebelli[1], Ioannis Ieropoulos [2], John Greenman [2], Chris Melhuish [2] and Tom Ziemke[1]

[1]University of Skövde, Cognition and Interaction Lab, Sweden
[2]University of West England, Bristol Robotics Lab, UK

Abstract

We present an evolutionary robotics investigation into the metabolism constrained homeostatic dynamics of a simulated robot. Unlike existing research that has focused on *either* energy *or* motivation autonomy the robot described here is considered in terms of *energy-motivation autonomy*. This stipulation is made according to a requirement of autonomous systems to spatiotemporally integrate environmental and physiological sensed information. In our experiment, the latter is generated by a simulated artificial metabolism (a microbial fuel cell batch) and its integration with the former is determined by an *E-GasNet*-active vision interface. The investigation centres on robot performance in a three-dimensional simulator on a stereotyped two-resource problem. Motivation-like states emerge according to periodic dynamics identifiable for two viable sensorimotor strategies. Robot adaptivity is found to be sensitive to experimenter-manipulated deviations from evolved metabolic constraints. Deviations detrimentally affect the viability of cognitive (anticipatory) capacities even where constraints are significantly lessened. These results support the hypothesis that *grounding* motivationally autonomous robots is critical to adaptivity and cognition.

Introduction

The pursuit of imbuing robots with levels of autonomy has resulted in recent emphasis on internal dynamics of robotic systems as they affect adaptive and cognitive behaviour (cf. Parisi 2004, Ziemke and Lowe 2009). McFarland (2008) has identified three core levels of autonomy – *energy*, *motivation* and *mental* levels and suggests: "Autonomy implies freedom from outside control. There are three main types of freedom relevant to robots. One is freedom from outside the control of energy supply. Most current robots run on batteries that must be replaced or recharged by people. Self-fuelling robots would have energy autonomy. Another is freedom of choice of activity. An automaton lacks such freedom, because either it follows a strict routine or it is entirely reactive. A robot that has alternative possible activities, and the freedom to decide which to do, has motivational autonomy. Thirdly, there is freedom of 'thought'. A robot that has the freedom to think up better ways of doing things may be said to have mental autonomy" (McFarland 2008, p.15).

Naturally, how the robot designer is to seamlessly integrate these levels of autonomy represents another challenge but inspiration can be derived from biology. A key feature of biological autonomous systems is homeostatic regulation. Drawing from Cannon (1915), the importance of bodily 'essential' variables to behavioural dynamics was identified in an artificial systems context by Ashby (1960). Ashby's *homeostat* produced feedback signals following deviation from a pre-set range of the essential variables (*EV*s). While Ashby's notion was deliberately abstract, biological evidence for the effects of *EV*s on regulation of behaviour has recently been found regarding feeding and drinking. Canabal et al. (2007) discovered that levels of extra cellular glucose in hypothalamus can impact on neural activity via slow diffusing nitric oxide (NO) molecules. NO emissions in glucose-sensitive cells correlate with feeding (cf. Morley et al., 1999) while 'osmoreceptor' cell NO emissions in hypothalamus correlate with drinking (cf. Yao et al. 2005).

Robot controllers have utilized bio-inspired mechanisms for 'brain-body' interfacing in the areas of: navigation (Vargas et al. 2009), foraging (McHale and Husbands 2006), two-resource problems (Avila-Garcìa and Cañamero 2004). This work has, however, invariably abstracted away details of the dynamic grounding of brain-body interfacing. Specifically, metabolic dynamics and their imposed behavioural constraints have been ignored. Instead, emphasis has been placed on motivation-like states (cf. McFarland and Spier 1997) as a function of *abstract* internal (essential) variable, and externally sensed, information. Such states are typically non-grounded either evolutionarily or metabolically. The resulting homeostatic expression of such robots may, therefore, be critically constrained regarding adaptive behaviour in spatial-temporal realistic environments.

Research into metabolic performance constraints has been carried out in recent years in the form of microbial fuel cell (MFC) robotics applications (cf. Melhuish et al. 2006, Ieropolous et al. 2007). MFCs can provide wheeled robots with (electrical) energy for driving motors as constrained by bio-chemical *EV* dynamics. MFC technology has the capacity to produce bioelectricity from virtually any unrefined

renewable biomass (e.g. wastewater sludge, ripe fruit, flies) using bacteria; thus, when used as the power source for actuation MFCs equip robots with a degree of energy autonomy concerning choice of 'recharging' resource. A limitation of artificial metabolism motored robots such as *EcoBot* (cf. Melhuish et al. 2006) given the present state of the art, however, is the energy requirement for actuating motors. Consequently, the robot may take as long as 15 minutes to move 15mm. This renders experimentation with new forms of homeostatic control and performance optimization challenging. A need is evident for simulations based scenarios for assessing the potential development of metabolism constrained robotic behaviour.

In the rest of this article we will describe an initial investigation into the dynamics of a robotic system that integrates two levels of autonomous control – *energy-motivation*. Two themes address the influence of simulated metabolic constraints on: 1) evolved sensor-motor resource acquiring strategies, 2) the emergence of affective ('motivational') dynamics. Spatiotemporal coherence between *internal* and *sensorimotor* domains is evaluated as it renders adaptive and cognitive behaviour. In the next section we introduce the components of the *energy-motivation autonomous robot* and our methodological approach. The results section evaluates themes 1) and 2) according to a comparative case study of best evolved controllers. The discussion section includes reference to present and future work.

Robot Architecture and Methodology

There are three architectural components: 1) a brain-body interface (*E-GasNet*) between 2) artificial metabolism (MFC model), and 3) sensorimotor (active vision) system. Below, each component is described in turn followed by the methodology used to assess the spatiotemporal coherent integration of the three components to adaptive behaviour.

Robot Architecture: The E-GasNet

The neurophysiological controller we propose is an extension of the GasNet (Husbands et al. 1998). The essential components comprise a standard neural network the activity of which is modulated by nitric oxide (NO) emissions enabling a spatiotemporal dynamic that when embedded in a wheeled robot tunes network performance to task requirements (cf. Smith et al. 2002). Work has been carried out utilizing GasNets according to evolutionary robotics investigations on bodily homeostasis (cf. Vargas et al. 2009) and energy constraints (cf. McHale and Husbands 2006). The focus, however, has not been on the incorporation of non-neural bodily states into GasNet 'nervous system' activity.

Based on the neuroscientific findings referred to in the previous section, we propose the *E-GasNet* ('Essential Variable Monitoring GasNet') as a type of GasNet developed according to an evolutionary robotics approach. The novel feature it incorporates is the use of *EV* level sensing nodes

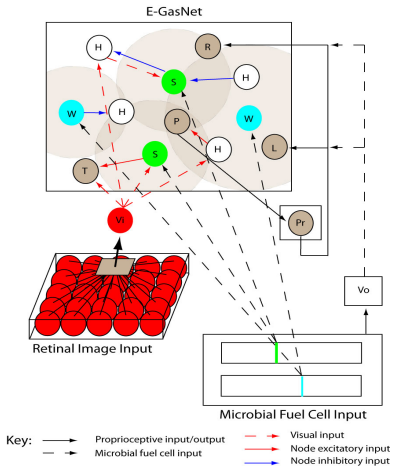

Figure 1: E-GasNet component of the complete energy-motivation autonomous robot architecture. Nodes: H = hidden, L = left motor, R = right motor, P = pan, T = tilt, V_i = Visual input, Pr = pan proprioception, W = water sensitive e-node, S = substrate sensitive e-node, V_o = MFC voltage input. Grey shaded circles depict potential e-node gas emissions. Green and blue coloured vertical lines provided by MFC represent substrate and water levels, respectively.

(for water and metabolizing-substrate) that emit gas contingent on the state of concomitant *EV*s. We term these nodes *e-nodes*. The E-GasNet (fig.1) represents the interface between artificial metabolic *EV* dynamics and actuators – (left and right) motors and active vision (pan and tilt) nodes. Depending on topological positioning on the two dimensional plane motor nodes in the network are modulated only by a retinal pan proprioception node and gas modulation – this simplified analysis concerning comparative sensorimotor activity. Pan and tilt nodes are modulated by electric input and gas. Electric input permits transient retinal image positioning on the camera. The position of nodes on the plane, the number of e-nodes and the sign and connectivity are determined by a genetic algorithm or GA (see methodology). An E-GasNet consists of four actuator nodes, four 'hidden' nodes and a variable number of e-nodes. E-nodes emit gas modulating the electric activity of neighbouring nodes (within a genetically specified radius) via affecting the gain of the output function. Gas emissions are dependent on a genetically determined e-node specific *EV* threshold. *EV* values are provided by the MFC dynamics (see next sub-section). Hidden nodes do not emit gas. Output from the MFC gates motor wheel activity while an output from a visual node provides a mean value of all cells on a 'retina' which inputs to the network as it pans and tilts across the camera image. The E-GasNet dynamic is governed by the same set of difference equations utilized by Husbands et al. (1998) and, where slightly adapted, Smith et al. (2002). It is to these papers that the reader is referred for details of electric output and gas emission dynamics.

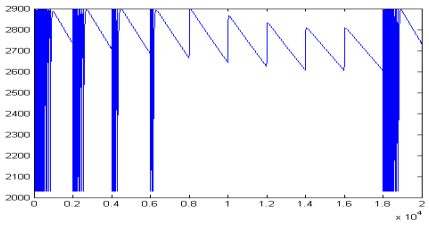

Figure 2: MFC model of system level (electric) energy output dynamics. The vertical axis provides output voltage (mV) where 2900 is the discharge level providing energy to the actuators (e.g. motors), the horizontal axis represents time in arbitrary units.

Robot Architecture: Artificial Metabolism

This component is comprised of the Microbial Fuel Cell (MFC) model of Montebelli et al. (2010a), designed at a level of abstraction purpose-made for autonomous robotics investigations. Critical to energy-motivation autonomous level integration is the charge-discharge electric output dynamics that gate motor wheel activation. An example of this dynamic is illustrated in figure 2 according to a substrate exhaustion cycle. At a threshold of electricity storage at the MFC capacitor bank (pre-set to 2900mV) energy is utilized by motors that indirectly contribute to the maintenance of the charge-discharge dynamic, i.e. through feeding/drinking. After a period without substrate, the charge is not arrived at in spite of periodic rehydration (every $0.2*10^4$ time units) at the cathode. Re-establishment of an efficient output dynamic owes to simulated fuel source provision at $1.8 * 10^4$ at the anode. This cycle demonstrates the requirement for *both* water and substrate (*EV*s) to be replenished for efficient system level energy to be produced. Reduced charge rate ensures less energy for the motors.

In the set-up used in our investigation, the robot produces a pulsing motor behaviour similar to 'EcoBot' (cf. Melhuish et al. 2006). This entails energy being made available to the motors for a short time window following the point of discharge. Where MFC performance degrades, motor pulses slow and in turn MFC performance continues to degrade as resource acquisition capacity is impaired. If the discharge threshold is not reached, motor output eventually ceases – no such constraint has been placed on visual sensing at present. For specific values used in our experimentation and an alternative application see Montebelli et al. (2010b).

The E-GasNet is evolved to track the level of the *EV*s in the MFC model – the GA may 'select' for e-nodes that 'monitor' the level of either substrate or water according to a genetically determined threshold value specific to the particular node. If the *EV* level falls below such a node-specific threshold, gas emission is initiated and linearly increments to an upper bound; only when *EV* values are re-established above threshold (as set by the GA) does the gas level linearly dissipate. In this Ashby-like manner, e-node activity

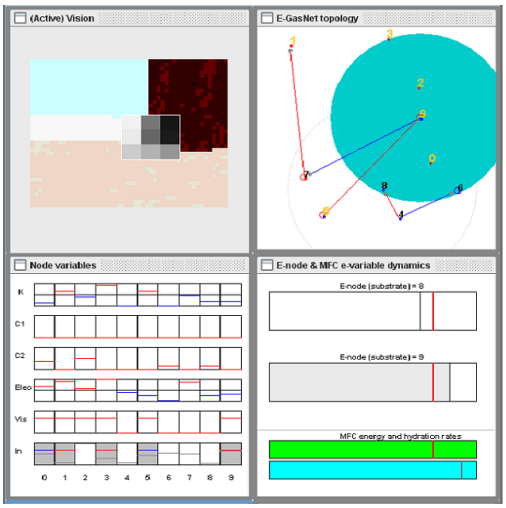

Figure 3: Controller dynamics top-left: retina superimposed on camera image, top-right: E-GasNet topology – blue circle represents (inhibitory) gas emission at node 9, bottom-left: E-GasNet parameters – K is gain level; $C1/C2$ are gas 1/2, respectively; $Elec$ is the electric output of each network node; vis is the scalar input from the retina (here 3*3 units); In is actual visual input, i.e. above noise threshold ensuring a differentiated node response to visual input, bottom-right: *EV* dynamics of the MFC including the same dynamics as they relate to e-node gas emission thresholds.

serves to anticipate the effect that *EV* depletion will have on the 'life-energy' output of the MFC providing a mode of embodied cognition. This occurs since MFC electric output cycles depend absolutely on efficient regulation of these two *EV*s. The e-node gas emission is the means by which body can interface with sensor-motor activity in order to pre-empt catastrophic performance degradation.

Robot Architecture: Sensor-Motor Morphology

An E-puck robot simulated in Webots (*Cyberbotics Ltd.* – *http://www.cyberbotics.com*) was used but any simple wheeled robot may be suitable. Our emphasis is on *integration* of sensorimotor capacities with neurophysiological dynamics. Sensor input consisted of a low dimensional grey-scaled retinal image superimposed on an e-puck camera image. The 'retina' is initialized for each evaluated robot controller in the centre of the camera image but may pan and tilt through 360 ° within the 2D bounds. Pan/tilt values (one node each) for the retina are modulated through: electric inputs from E-GasNet nodes, gas, a pan proprioception node. This permits a type of *active vision* similar to Floreano et al. (2004). A retinal scalar value inputs to GA-determined nodes in the network. Figure 3 provides a snapshot of the robot graphical interface for the retinal network (along with E-GasNet topology/activity and *EV* dynamics).

The equations that determine the active vision effects on robot dynamics are as follows: $P_o(t) = (C_x + R_w/2) - C_w/2$ and $P_r(t) = P_o(t-1)/(C_w - R_w)$ where $P_o(t)$ = pan

orientation at time t, C_x = x axis value of the robot camera image in [0,50], R_w = retina width genetically determined in [15,25], C_w = camera image width (50 pixels); $T_o(t) = (C_y + R_h/2) - C_h/2$ where $T_o(t)$ = tilt orientation at time t, C_y = y axis value of the robot camera image in [0,40], R_h = retina height genetically determined in [12,20], C_h = camera image height (40 pixels); $P_r(t)$ = pan proprioception at time t. Motor wheel output is determined by: $O_i(t) = b_r*(\alpha+P_r(t-1)*(V_i > V_ti)*(V_i-V_ti))$ where O = wheel output for node $i \in \{1,2\}$ at time t, b_r = 'burst' boolean, α = a constant set at 0.5, V = retina input in [0,1], V_t = a genetically determined node-specific threshold in [0,0.5].

Methodology: The Two Resource Problem

The *energy-motivation autonomous robot* was evaluated according to a two resource problem (McFarland and Spier 1997) where applicable resources are water and fuel substrate. The literal use of two resources (one of each type) serves as an initial benchmark control to facilitate identification of core principles and homeostatic dynamics. The two resource paradigm is a class of problem whereby *adaptive* sensorimotor activity enables a (quasi) optimal trade-off between two conflicting *EV* needs. Spier (1997) studied two-resource problems on 2D scenarios for agents utilizing an ethology-based *cue-deficit model* that states that likelihood of enacting a 'motivated' behaviour in animals is determined by the product of: 1) external stimuli, 2) related physiological need deficit. The realization of such a cue-deficit model in a 3D world is not obvious particularly if the robot sensors do not provide pre-given information with which to discriminate stimuli or/and implicitly provide information regarding stimulus distance/attainability. A stronger measure of autonomous capabilities is provided by robots remaining viable over long periods in partially human-known environments, possibly inhospitable to human habitation. Energy autonomous robots flexible in their means of refuelling are critical in this case. Realistic metabolic constraints impact on sensorimotor capabilities rendering high-level modelling approaches compromised regarding robot adaptivity to dynamic and challenging environments. Situated *integration* of internal and external sensing is therefore needed in order to enable motivational autonomous capabilities.

Evolved E-GasNet interfacing of metabolic and sensorimotor activity provides a spatiotemporally and metabolically situated cue-deficit model apt for 3D world robot performance where resource-specific sensory information concerning distance and type is not explicitly pre-given.

Methodology: An Evolutionary Robotics Approach

100 candidate controllers were evaluated over 50 generations via the distributed GA used by Husbands et al. (1998). Each evaluation consisted of a robot making 20 selections (one per trial) from the 2 available resources. Each trial is terminated either by successfully reaching a resource leading to instantaneous related *EV* replenishment, or if a resource is not reached by 500 cycles (basic timestep = 64ms). The latter time constraint ensured against inefficient/arbitrary approach behaviours. The metabolic constraints required the robot to 'switch' preference from one resource to the other at least twice ensuring against evolution of uninteresting dynamics. Agents viable after 20 trials were considered *survivors*. Both resources were within camera image scope at the beginning of each trial to limit potential bias towards one or other resource – test trials found no observable bias. Water and substrate resources were placed left and right of the robot trial starting position, respectively. This positioning – relative to the centre of the robot – was not varied in order to promote ease of analysis of the complex interactive dynamics of the system. Solutions were analyzed according to an independent variable (IV) – clamping, or not, of gas effects on motor node activity; the IV, thus, consisted of two values - a) Gas modulated motor output (*GM*), b) Non-gas modulated motor output (*NGM*). In a) motor output could be affected both by gas and the pan proprioception node; in b) motor output was modulated only by the pan proprioception node – this exerted evolutionary pressure for the emergence of 'active vision' strategies while purely electric inputs to the retina position otherwise ensured early stabilization. The only means by which robots can survive trials is by switching from one resource preference to the other over the 20 trials. This switching in the latter condition can, therefore, *only* be achieved via e-node gas modulation of pan-tilt activity. The emergence of e-node arbitration is therefore unsurprising. Our investigation instead focuses on exactly how such arbitration dynamically occurs.

The evaluation criteria consisted of 1) fitness, 2) no. *survivors*. Robot fitness is defined: $fit(t) = fit(t-1) + (subst(t) + wat(t))/2$ and $fit_\mu = t_{term} * (fit(t)/N_{tr})$ updated once per trial at time t, t_{term} is a boolean determining termination of the controller evaluation, i.e. at the end of N_{tr} = 20 trials. The fitness function captures physiological state at the time of resource acquisition while no assumptions concerning *ideal* state are made. Evolutionary parameters adhered to Husbands et al. (1998) but adopted the gaussian gas diffusion of Smith et al. (2002) and the connectivity schema of Jakobi (1998). Further parameters subject to the GA were: e-node no. (in [0,6]), e-node gas emission thresholds (in [0.0,1.0]), retina squared unit dimension size (in [3,5] where a unit = 5*4 pixels and camera dimensions are fixed at width = 50, height = 40). Finally, unlike the classical GasNet, left/right wheel (and pan/tilt) nodes' x, y coordinates were evolutionarily specified.

Results

Evolution and Evolvability of Strategies

Figure 4 illustrates fitness and survivor rate of all controllers over 10 runs. Evaluation of independent sample t-tests indicated that robots were significantly fitter in early generations

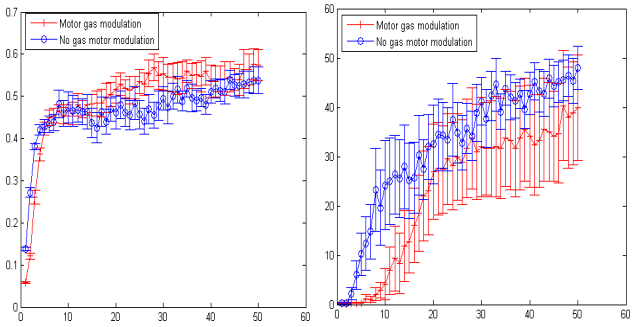

Figure 4: Left: Fitness (in [0.0,1.0]). Right: Survival rate. Mean values for agent popn. over 50 generations comparing gas modulating motor activity (*GM*) to non-gas motor modulating (*NGM*) runs; Error bars calculated as: $SE = \frac{sd}{\sqrt{N}}$ where N = 10 runs.

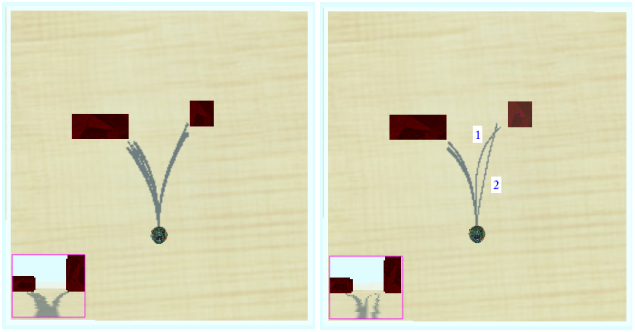

Figure 5: Inter-trial motor trajectories – inset camera images show in-trial perspectives. Left: *GMC* trajectories (20 trials). Right: *NGMC* trajectories (for visibility – trial 1 and 2, and a sub-set).

(1-4) of *NGM* runs than they were in *GM* runs. Comparison of performance of survivors uncovered that only generations 5, 7-9 produced significant differences with higher survivor rate in *NGM* runs. All tests were at $p < 0.05$ for two-tailed tests with d.o.f = 18. These results suggest a tendency, early in evolution, to favour higher performance in *NGM* runs suggesting greater evolvability. However, allowing motor nodes to be potentially modulated by gas emissions in *GM* runs ensured additional genome complexity possibly requiring more generations for adaptive strategies to manifest. The high survival variance in *GM* runs – 3/10 runs produced no survivors by generation 50 – compared to 10/10 in *NGM* runs producing > 30 survivors by generation 50 – and higher mean in *NGM* runs hints at *NGM* strategies differentiable from those found in *GM* runs.

MFC Constraints: A Comparative Case Study

An in-depth evaluation of individual controllers taken from the best runs of each condition furnished a case study comparison in order to unveil adaptive strategies. Owing to evolution converging on a common ancestor by generation 50 a given controller selected from the *genome candidate solution grid* (see Husbands et al. 1998) provided a typical evolved topology for the run. We compared only viable controllers, i.e. ones that enabled robots to 'survive' 20 trials.

Figure 5 depicts trial-by-trial motor trajectories for the two controllers. On the left of the figure is the *GM* controller (*GMC*). Typically, per trial, the robot followed an arced path towards the nearest edge of the approached resource which is energy-efficient. On the right of the figure is the *NGM* controller (*NGMC*) showing a similar pattern of approach for the water resource (left-side) but more varied trajectories for substrate approach (right-side). Substrate is acquired on 4/20 occasions (compared to 7/20 for the *GMC*). On trial one the robot retina is biased, by electric inputs to pan/tilt nodes, towards water resource saccade-fixation but pans to substrate subsequent to gas modulation effects. Figure 5 (right) depicts this initial movement towards the water which then arcs towards the substrate. On trial two, the robot decisively approaches the substrate where the retina remains fixated while the gas dissipates. Regarding *NGMC*, expression of 'opportunism' (trial 1) and 'persistence' (trial 2) is afforded by *active vision*. Such modes of flexible foraging activity have been posited as expressions of motivated behaviour in non-metabolically grounded architectures tested on two-resource problems (cf. Spier 1997, Avíla-García and Cañamero 2004). Opportunism entails ability to "change one's mind" concerning a preference while persistence entails behavioural resistance to alternative motivations. These behaviours accord with McFarland's (2008) *non-reactive* criterion for motivational autonomy. Such flexibility is afforded owing to fast saccade-fixation speed relative to inter-pulse wait time providing an example of how such system level energy constraints may be exploited sensorially given low, or, in the case of the robots here, zero, energy constraints to saccade. In essence, during the waiting period, the robot is able to saccade to the 'desired' resource affording *anticipatory* activity. Regarding *GMC*, the *orientation behaviour*, is more *reactive* – the tight coupling between metabolic and motor activity ensures behaviour is tied to present state (the inter-pulse wait time is not exploited – the retina remains, mostly, static). The comparative metabolic under-determination of sensor-motor activity in *NGMC* behaviour might permit us to label it cognitive (see Barandiaran and Moreno 2008). In spite of its cognitive utility, the emergence of active vision strategies appears to be stifled in the *GMC* condition and to no apparent advantage. This appears to owe to the relative ease of evolution to tap and fine-tune motor orientation-based solutions creating an obstacle for active vision evolutionary transition.

Internal and Sensorimotor Dynamics In order to provide a mechanistic explanation of how metabolism constrains sensorimotor strategies we investigated *sensorimotor* and *internal* dynamics as they affected resource selection. In figure 6 are displayed the evolved topologies for our study. In both cases, multiple gas-emitting e-nodes (grey-circled)

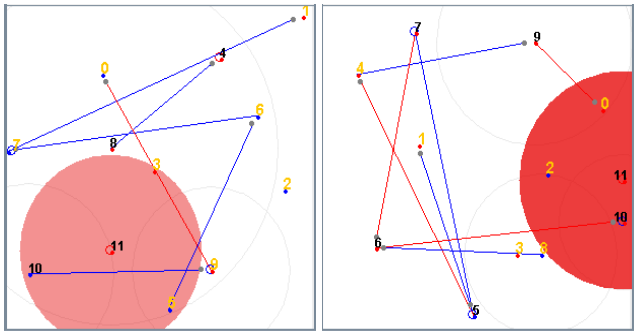

Figure 6: Topology of evolved controllers. Left: *GM* controller. Right: *NGM* controller.

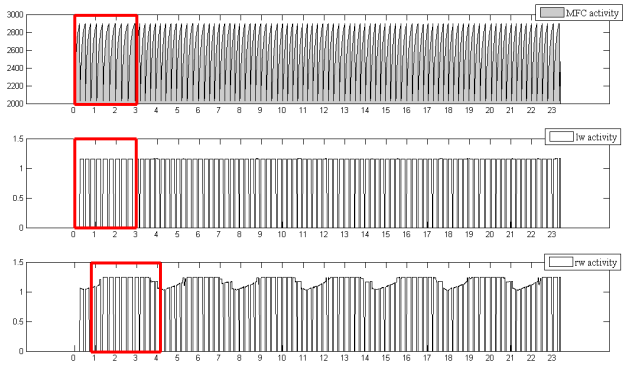

Figure 7: MFC-constrained sensor-motor activity for *GM* controller over 20 trials on a normalized time scale.

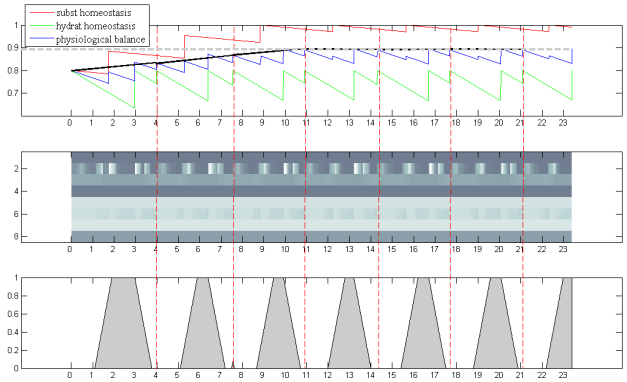

Figure 8: Internal activity for *GM* controller over 20 trials. Top: Physiological (*EV*) balance. Middle: E-GasNet electric activity (4 hidden nodes, 4 e-nodes). Bottom: E-node 11 gas dissipation.

evolved. However, via systematic 'clamping' of gas emission capability it was found that both controllers functionally depended on only a single e-node. The left side (*GMC*) shows that only the right wheel (node 3) is directly affected by gas (e-node 11). Left wheel (1) and pan (0) nodes are only indirectly gaseously affected while the tilt node (2) is affected only by sensory input (indicated by yellow figure colouration). The right side (*NGMC*) shows both pan and tilt nodes within the e-node (11) gas emission radius. This implicates gas as a motor switch mechanism where for *GMC* and *NGMC* the individual e-nodes are sensitive to water and substrate, respectively. The *GMC* was observed on individual re-runs not to use active vision. Figure 7 displays over the 20 trials *GMC* motor activity in [0,0.5] where a constant $C = 0.75$ was added to ensure forward movement (given sufficient MFC-supplied energy). The boxed windows capture a transient phase prior to a more regular periodic dynamic. MFC charge-discharge cycles slow during this period as does left and right wheel pulsed activity. The increased output of the right wheel captured in a time-lagged window reflects slow diffusing gas emission effects consistent with a water resource orienting response. The slow gas dissipation ensures 'commitment' in *GMC* accounting for a water-substrate acquisition ratio of 2:1 – the robot chooses water a second time even after acquisition brings the *EV* value above the e-node gas emission threshold.

Figure 8 displays *GMC internal dynamics* for: *EV*s (top), E-GasNet electric activity (middle), e-node gas output (bottom). Periodic activity for gas output at the e-node arises after the previously described transient phase. Vertical red dashed lines capture windows of resource acquisition dynamics comprised of 3 selections at the 2:1 ratio for water:substrate. The dashed horizontal grey line depicts the stable (mean) *EV* balance and it can be observed with reference to the skewed horizontal black line linking *EV* balance windows that stability occurs after 3 windows. During this period the robot's initial *EV* values become increasingly well regulated therefore. On the other hand, a salient periodic gas emission (and GasNet electric activation) dynamic appears prior to this – after the first window – in accordance with water acquisition dynamics. This happened in spite of the fact that resource distance from the invariant initial position of the robot was varied (to prevent strong sensor-motor dependencies – see Jakobi 1998). The duration of gas emission activity in the e-node observably correlates with the undulating right wheel activity responsible for 'behavioural switching' (fig.7) and dissipates at the point of water resource acquisition. Substrate approach, in the absence of gas effects, is the default behaviour – this is reversed for the *NGMC*. The gaseous 'thirst' signal is affective insofar as it is evolutionarily and metabolically grounded into the agent-environment dynamic and the product of embodied (e-node) anticipatory activity. In sum, the two controller strategies use gas for *EV*-relevant switching from a default resource-orientation response to spatiotemporally-tuned orientation towards the alternative resource. This 'tuning' is critical to sustaining the internal-sensorimotor cohesion of the robot. To better establish the relevance of metabolic grounding to this cohesion we varied inter-pulse wait time (MFC system level constraint) and re-assessed performance of the controllers.

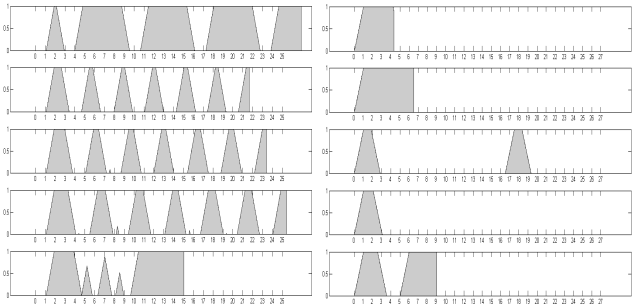

Figure 9: Gas emission as modulated by metabolic constraints over 20 trials according to $bC = \{0, 50, 75, 100, 150\}$ where constraints are represented top to bottom according to ascending strengths. Left: *GM* controller, Right: *NGM* controller.

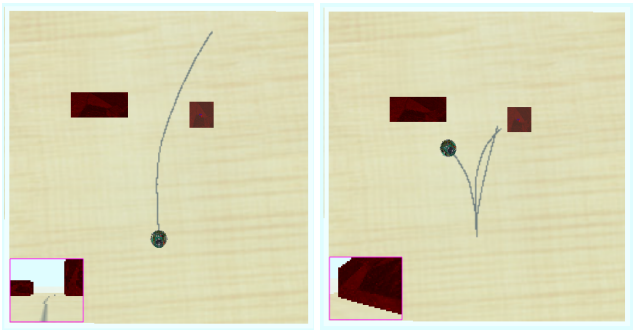

Figure 10: *NGMC* motor trajectories at different metabolic constraints. Left: low *intermediate* – the robot is not viable beyond one trial. Right: high *intermediate* – the robot stops moving (is non-viable) following two successful resource acquisitions.

Dynamic Robustness to MFC constraints The inter-pulse wait time is determined by a constant/parameter bC. All controllers were evolved according to $bC = 75$ steps. This was chosen as an apt challenge level following pre-trial testing. The two evolved controllers in the case study were tested against $bC\epsilon\{0, 50, 75, 100, 150\}$ providing *zero*, *intermediate* (50,75,100) and *high* (150) constraints, respectively. Figure 9 provides gas emission plots over all trials for the two evaluated controllers. It is observed for the *NGMC* (right-side) that only at the constraint value on which it was evolved does it remain viable – robots 'die' at the gas vertical 'cut-off' point and must emit at least twice – perform two switches – over all trials. Interestingly, at *zero* and low *intermediate* constraints the robot fairs badly but performs relatively better at high *intermediate* and *high* constraints. Figure 10 illustrates why this is the case. On the left-side (low *intermediate* constraint), saccade-fixation activity is now insufficiently fast relative to motor speed. The robot behaves 'opportunistically' but receives insufficient retinal stimulation to fixate on the substrate leading to 'dis-orientation'. On the right-side, the high inter-pulse wait time allows saccading to the substrate. This behaviour is more efficient than at the bC value on which the controller was evolved. However, owing to the strong constraint and requirement for regular rehydration the robot soon becomes unviable.

The internal dynamics of the *GMC* (fig.9 – left) are equivalent for all *intermediate* constraints with the same resource choice profile over the 20 trials. Interestingly, at the *zero* constraint the dynamic pattern of gas emissions bifurcates, relative to *intermediate* constraints, early in the trial set. This is an example of robot 'dithering' between the two resources leading to no resource acquisition on trial two which, following the initial transient, periodically recurs. This dynamic is viable but sub-optimal – the robot controller was evolved on $bC = 75$ and whilst robust to relatively minor bC *intermediate* shifts, dynamics are non-robust to extreme shifts of the metabolic constraint. The use of a sub-optimal strategy given a *zero* constraint is viable since the robot only 'dies' following a full trial of non-movement. MFC degradation is not sufficient for this to occur owing to the relatively unchallenging agent-environment dynamic.

In summary, we can say that the challenge level of the environment alone is an insufficient indicator of likely robot viability. It is more informative to consider the robot's spatiotemporal cohesion given internal and sensorimotor domains and evolved metabolic grounding. Specifically, 'dithering' in the *GMC* at *zero* metabolic constraint is an example of maladaptive behavioural performance not present at the evolved constraint. The above highlights the requirement for autonomous robotics architectures to account for metabolic grounding in order to shape adaptive and cognitive (anticipatory) capacities. Affective signals are critical for cohering body-brain dynamics and may be robust to perturbations in agent-environment coupling but are rendered ineffectual if the integration of internal and sensorimotor robotic domains is insufficient.

Discussion

This paper has described work towards an autonomous robotic system focused on the *integration* of energy and motivation autonomous levels as described by McFarland (2008). We suggest that top-down (e.g. ethological) models claiming to implement motivational autonomy in robots are limited as they: 1) ignore how metabolic constraints impact on sensorimotor activity, 2) require a priori environment knowledge. A major application for autonomous robots, however, is in their deployment in inhospitable and unknown environments where harmonious spatiotemporal agent-environment integration is crucial for long-term viability. Our work presents the first steps towards integrating levels of autonomy hinting at the potential for adaptive cognitive behaviour to emerge out of metabolic constraints. We summarize our findings as follows:

1. Two strategies evolutionarily emerged that spatiotemporally integrated metabolic and sensorimotor activity.

2. Strategy one – active vision – enabled robots to exploit the energy-constrained pulsed motor behaviour to produce:
   (a) Sensorial anticipatory behaviour,
   (b) Energy-efficient motor trajectories,
   (c) Adaptive opportunistic-persistent behaviours.
3. Strategy two – motor orientation – did not sensorially exploit its energy-constrained motor-pulsed behaviour.
4. *E-nodes*, via *EV*-level thresholded gas emission, anticipate metabolism constrained performance degradation.

The grounding of behaviour according to artificial metabolic constraints permitted the evolution of sensorial anticipatory behaviour in the form of simple pan/tilt active vision. Interfacing 'body' (MFC) and 'brain' (*E-GasNet*) entailed tuning gas emissions to enable this anticipatory sensorimotor response. Stable gas emission dynamics in functional nodes when metabolically situated constitutes motivation-like (thirst/hunger) signals. The existence per se of such signals precipitates orientation/saccade switching and is functional therein. The periodicity and duration of such signals are requisite to the agent-environment dynamic niche and functional therein. A significant change to this dynamic, e.g. severe modification of the metabolic constraint, renders the motivation-like signals non-adaptive even if the task challenge is effectively reduced.

We are currently investigating 'naturalistic' settings with dynamic resource configurations. Early findings hint at the emergence of distributed forms of e-node networks adapted to this more complex dynamic. A long term aim is to unveil robot controllers that exhibit *energy-motivation-mental autonomy* (see Ziemke and Lowe 2009) described using utility- and optimality-based ecological models.

Acknowledgements

This work has been supported by a 2006-2009 EC grant to the FP6 project "Integrating Cognition, Emotion and Autonomy" (ICEA, IST-027819, www.iceaproject.eu).

References

Ashby, W.R. (1960). *Design for a brain: The origin of adaptive behaviour*. Chapman and Hall.

Avíla-García, O. and Cañamero, L. (2004). Using hormonal feedback to modulate action selection in a competitive scenario. In *From Animal to Animats 8: Proc. of the 8th International Conference on Simulation of Adaptive Behaviour*. Cambridge, MA: MIT Press, 243-252.

Barandiaran, X. and Moreno, A. (2008). Adaptivity: From Metabolism to Behavior. *Adaptive Behavior*. 16: 325-344

Canabal, D.D., Song, Z., Potian, J.G., Beuve, A., McArdle, J.J. and Routh. V.H. (2007). Glucose, insulin, and leptin signaling pathways modulate nitric oxide synthesis in glucose-inhibited neurons in the ventromedial hypothalamus. *Am. J. Physiol. Regul. Integr. Comp. Physiol.* 292:1418-1428.

Cannon, W.B. (1915). *Bodily Changes in Pain, Hunger, Fear and Rage*. Appleton, New York.

Floreano, D., Kato, T., Marocco, D. and Sauser, E. (2004). Coevolution of Active Vision and Feature Selection. *Biological Cybernetics*. 90(3):218-228.

Husbands, P., Smith, T., Jakobi, N. and O'Shea, M. (1998). Better Living through Chemistry: Evolving GasNets for Robot Control. *Connection Science*. 10(3/4):185-210.

Ieropoulos, I., Melhuish, C. and Greenman, J. (2007). Artificial gills for robots: Mfc behaviour in water. *Bioinspiration and Biomimetics*. 2, S83-S93.

Jakobi, N. (1998). Minimal Simulations for Evolutionary Robotics. *DPhil thesis*, University of Sussex.

McFarland, D. (2008). *Guilty Robots, Happy Dogs*. Oxford University Press.

McFarland, D. and Spier, E. (1997). Basic cycles, utility and opportunism in self-sufficient robots. *Robotics and Autonomous Systems*. 20:179-190.

McHale, G. and Husbands, P. (2006). Incorporating Energy Expenditure into Evolutionary Robotics Fitness Measures. In L. Rocha et al. (Eds), *Proc. Alife X*, 206-212, MIT Press.

Melhuish, C., Ieropoulos, I., Greenman, J. and Horsfield, I. (2006). Energetically autonomous robots: food for thought. *Autonomous Robots*. 21:187-198.

Montebelli, A., Ieropoulos, I., Lowe, R., Ziemke, T., Melhuish, C. and Greenman, J. (2010a). Unplugged! A mathematical model of Microbial Fuel Cells for energetically self-sustainable simulated robotic agents. In preparation.

Montebelli, A., Lowe, R., Ieropoulos, I., Melhuish, C. Greenman, J., and Ziemke, T. (2010b). Exploring prospective hybrid life: Microbial Fuel Cell driven behavioral dynamics in robot simulations. *Artificial Life 12*, in press.

Morley, J.E., Alsaher, M.M., Farr, S.A., Flood, J.F. and Kumar, V.B. (1999). Leptin and neuropeptide Y (NPY) modulate nitric oxide synthase: further evidence for a role of nitric oxide in feeding. *Peptides*. 20:595-600.

Parisi, D. (2004). Internal robotics, *Conn. Sci.*, 16(4):325-38.

Smith, T., Husbands, P., Philippides, A. and O'Shea, M. (2002). Neuronal Plasticity and Temporal Adaptivity: GasNet Robot Control Networks. *Adaptive Behavior*. 10(3-4):161-183.

Spier, E. (1997). *From Reactive Behaviour to Adaptive Behaviour*. PhD Thesis. University of Sussex.

Vargas, P., Moioli, R.C., von Zuben, F.J. and Husbands, P. (2009). Homeostasis and evolution together dealing with novelties and managing disruptions. *International Journal of Intelligent Computing and Cybernetics*. 2(3):435-454.

Yao, S.T., Gouraud, S., Paton, J.F.R. and Murphy, D. (2005). Water Deprivation Increases the Expression of Neuronal Nitric Oxide Synthase (nNOS) but Not Orexin-A in the Lateral Hypothalamic Area of the Rat. *The Journal of Comparative Neurology*. 490:180-183.

Ziemke, T. and Lowe, R. (2009). On the Role of Emotion in Embodied Cognitive Architectures: From Organisms to Robots. *Cogn. Comp.*,1:104-117.